Check for updates

Geophysical Research Letters

RESEARCH LETTER
10.1029/2025GL118170

Monitoring Source Areas of Post-Fire Geomorphic Processes Using an In Situ Multi-Sensor System

N. Dematteis[1], L. Pisano[2], R. M. Cavalli[3], M. Cavalli[4], S. Crema[4], M. De Biase[2], M. Donnini[3], S. L. Gariano[3], M. Piantini[4], M. Rossi[3], and G. Esposito[3]

[1]Research Institute for Geo-hydrological Protection (CNR-IRPI), Torino, Italy, [2]Research Institute for Geo-hydrological Protection (CNR-IRPI), Rende, Italy, [3]Research Institute for Geo-hydrological Protection (CNR-IRPI), Perugia, Italy, [4]Research Institute for Geo-hydrological Protection (CNR-IRPI), Padova, Italy

Key Points:

- Advanced video cameras equipped with visible and thermal sensors are tested to detect post-fire geomorphic processes at source areas
- Soil water content, meteorological, and seismic data are also collected to investigate conditions leading to the initiation of processes
- During two nocturnal rain events, rockslides, earthslides, gully erosion, and sediment-laden flows were successfully detected in real time

Supporting Information:

Supporting Information may be found in the online version of this article.

Correspondence to:

L. Pisano,
luca.pisano@cnr.it

Citation:

Dematteis, N., Pisano, L., Cavalli, R. M., Cavalli, M., Crema, S., De Biase, M., et al. (2025). Monitoring source areas of post-fire geomorphic processes using an in situ multi-sensor system. *Geophysical Research Letters*, *52*, e2025GL118170. https://doi.org/10.1029/2025GL118170

Received 15 JUL 2025
Accepted 16 SEP 2025

Author Contributions:

Conceptualization: G. Esposito
Data curation: N. Dematteis, L. Pisano, R. M. Cavalli, M. Cavalli, S. Crema, M. De Biase, M. Donnini, S. L. Gariano, M. Piantini, M. Rossi, G. Esposito
Formal analysis: N. Dematteis, M. Cavalli, S. Crema, M. Donnini, S. L. Gariano, M. Piantini, M. Rossi, G. Esposito
Investigation: N. Dematteis, L. Pisano, R. M. Cavalli, M. Cavalli, S. Crema, M. De Biase, M. Donnini, S. L. Gariano, M. Piantini, M. Rossi, G. Esposito
Methodology: N. Dematteis, L. Pisano, R. M. Cavalli, M. Cavalli, S. Crema, M. De Biase, M. Donnini, S. L. Gariano, M. Piantini, M. Rossi, G. Esposito

© 2025. The Author(s).
This is an open access article under the terms of the Creative Commons Attribution License, which permits use, distribution and reproduction in any medium, provided the original work is properly cited.

Abstract Geomorphic processes that occur after wildfires in mountainous areas require a deep understanding due to complex interactions of fire effects with the landscape surface. In situ monitoring systems can support this task, even if some limitations that affect traditional sensors can hamper their action. The current work presents an advanced multi-sensor monitoring system composed of an all-in-one meteorological station, sensors to survey soil water content, a seismic station, and a pan-tilt-zoom video camera equipped with visible and thermal sensors enabling continuous monitoring of fire-affected sites. The experimental technological setup successfully documented the evolution of environmental conditions during intense rainfall events in southern Italy, able to trigger post-fire soil erosion and mass movements which were accurately detected by the system. Besides the successful outcomes demonstrating to overcome common drawbacks of in situ monitoring applications, we discuss research findings about the initiation mechanisms of the observed post-fire geomorphic processes.

Plain Language Summary Wildfires can change the stability of slopes in mountainous areas, but scientists still need to better understand how fire affects the ground and increases the risk of landslides and soil erosion. To help with this, we are testing a new field monitoring system at two wildfire-affected sites in southern Italy. The system includes weather sensors, soil moisture sensors, a seismic station, and a video camera with visible and thermal imaging. Together, these tools continuously monitor changes in the environment. During two heavy rainstorms, the system successfully captured evidence of erosion and small landslides, even at night. These early results show that our multi-sensor setup is a promising way to monitor geomorphic changes in burned landscapes and improve understanding of post-fire hillslope instability.

1. Introduction

Understanding geomorphic processes in recently burned landscapes is engaging multidisciplinary research teams worldwide. Approaches commonly used to investigate post-fire geomorphic processes are based on remote sensing and numerical models (Cao et al., 2024; Ellett et al., 2019; Ouyang et al., 2023; Pelletier & Orem, 2014; Rengers et al., 2019). The use of field monitoring systems is still limited, especially outside the USA where valuable applications are reported by Kean et al. (2011, 2012), Martinez et al. (2025), Porter et al. (2021, 2023), and Raymond et al. (2020). These studies provide examples of in situ hydrological and seismic monitoring of post-fire debris flows (Esposito et al., 2023; Gartner et al., 2005). Even if debris flow monitoring systems are not a novelty in the field of earth sciences (e.g., Hürlimann et al., 2019 and references therein), those focusing on source areas of also landslides occurring in burned landscapes are still uncommon. This is in contrast with the growing need for up-to-date knowledge on the initiation mechanisms of such processes. For example, the transition from rainfall-triggered surface erosion of burned soils (i.e., rilling or sheetwash) to high-magnitude debris flows, the spatial and temporal variability of post-fire sediment supply, relationships between burn severity levels and location of hillslope instability processes, are some of the research gaps that field monitoring systems might help to address (Tang et al., 2019).

Physical variables commonly selected to investigate initiation mechanisms of post-fire geomorphic processes are: (a) rainfall, (b) soil water content (SWC), and (c) pore water pressure. Accordingly, traditional sensors are tipping bucket rain gauges, time/frequency domain reflectometry (TDR/FDR) devices, tensiometers and pressure transducers, respectively (González-Pelayo et al., 2024; Kean et al., 2011, 2012). These sensors are often coupled with video cameras to obtain visual documentation of processes during the propagation stage, or with seismic

19448007, 2025, 19, Downloaded from https://agupubs.onlinelibrary.wiley.com/doi/10.1029/2025GL118170 by CochraneItalia, Wiley Online Library on [14/10/2025]. See the Terms and Conditions (https://onlinelibrary.wiley.com/terms-and-conditions) on Wiley Online Library for rules of use; OA articles are governed by the applicable Creative Commons License

Resources: M. Rossi, G. Esposito
Supervision: G. Esposito
Validation: L. Pisano, M. De Biase, M. Donnini, M. Piantini, M. Rossi
Visualization: N. Dematteis
Writing – original draft: N. Dematteis
Writing – review & editing: N. Dematteis, L. Pisano, R. M. Cavalli, M. Cavalli, S. Crema, M. De Biase, M. Donnini, S. L. Gariano, M. Piantini, M. Rossi, G. Esposito

sensors for their detection and characterization. Even if based on advanced technologies, all these sensors can be affected by strong limitations. The spatial representativeness of rainfall, SWC and pore water pressure, as well as the dimming of video footage of distant hillslopes during the night, or interpretation of seismic signals in noisy environments possibly prone to multiple geomorphic processes, may hamper the processes detection and reduce usefulness of the whole monitoring activity.

Modern technologies can provide new solutions to reduce technical drawbacks like these. In this framework, the current contribution presents a prototype monitoring system aimed at: (a) detecting post-fire geomorphic processes at source areas and (b) measuring environmental variables controlling their initiation. The system is being experimented in southern Italy, in sites struck by extreme wildfires and post-fire intense rainfall events that triggered different types of geomorphic processes.

2. Pilot Sites

We designed and installed two experimental monitoring stations at two pilot sites in the Calabria region, namely Roccaforte del Greco and Montebello Jonico (Figure 1). Both sites are located in the Aspromonte, a massif that rises from sea level to an elevation of 1,956 m a.s.l. Due to the extremely pervasive and intense tectonic deformation associated with deep rock weathering (Calcaterra & Parise, 2010), hillslopes of the Aspromonte massif are prone to different types of mass movements (Robustelli & Sorriso-Valvo, 2017). These can be triggered by intense rain bursts that in the area can exceed 100 mm in 1 hr, or by prolonged rainfall controlled by orography (Bombino, Barbaro, et al., 2024).

2.1. Montebello Jonico

The site of Montebello Jonico (Figure 1b) is a small-scale catchment (16 ha) providing quick hydro-geomorphic response to rain bursts. The morphology is characterized by local vertical cliffs and steep hillslopes with average slope angles of 30°. Gradients of the catchment floor are reduced by a dozen retention check dams, filled by sediments accumulated after their construction in the 70s. The monitoring system is installed on one of these dams, at an average distance of 450 m from the headwater (Figure 1b). Geology consists of metamorphic units formed by phyllites with intercalations of graphitic metapelites, overlayed by weathered sandy-matrix conglomerates including heterometric clasts up to a few cubic meters. In the summer of 2023, a wildfire burned through the Montebello catchment with moderate-low burn severity, reducing the vegetation cover consisting of grassland and Mediterranean shrubland. This wildfire was ranked as the largest in Italy in 2023.

2.2. Roccaforte del Greco

The site of Roccaforte del Greco represents a planar hillslope domain (Figure 1c). This has an extension of 4 ha, with an average slope angle of 37°. Some low-order channels are also present. The geological unit outcropping in the area is composed of heavily weathered and fractured phyllites and schists. In 2021, the selected hillslope was affected by an extreme wildfire that burned the low-lying vegetation with moderate-high burn severity (Bombino, D'Agostino, et al., 2024). Since the monitoring system is positioned on an opposing hillslope with similar geology, no variables are measured directly on the target hillslope located approximately 450 m away (Figure 1c).

3. Materials and Methods

3.1. Monitoring System Design and Data Communication

The designed monitoring stations (Figure 2) are equipped with: two 100 W-solar panels, a couple of metal boxes sheltering batteries, electric circuits, and a Campbell CR1000X datalogger. Additionally, 4G modem-routers coupled with high-gain antennas allow data transmission and remote management of the datalogger. Meteorological and SWC measurements are published on two proprietary web platforms, while the images are collected in cloud servers. Seismic data are not transmitted due to excessive size, requiring on-site download.

3.2. All-in-One Meteorological Sensor

Meteorological variables are measured with an all-in-one autonomous weather station, model Campbell ClimaVue™50. This station provides data of air temperature, relative humidity, vapor pressure, barometric pressure, wind (speed, gust, and direction), solar radiation, rainfall, and lightning strike (count and distance) every minute.

19448007, 2025, 19, Downloaded from https://agupubs.onlinelibrary.wiley.com/doi/10.1029/2025GL118170 by CochraneItalia, Wiley Online Library on [14/10/2025]. See the Terms and Conditions (https://onlinelibrary.wiley.com/terms-and-conditions) on Wiley Online Library for rules of use; OA articles are governed by the applicable Creative Commons License

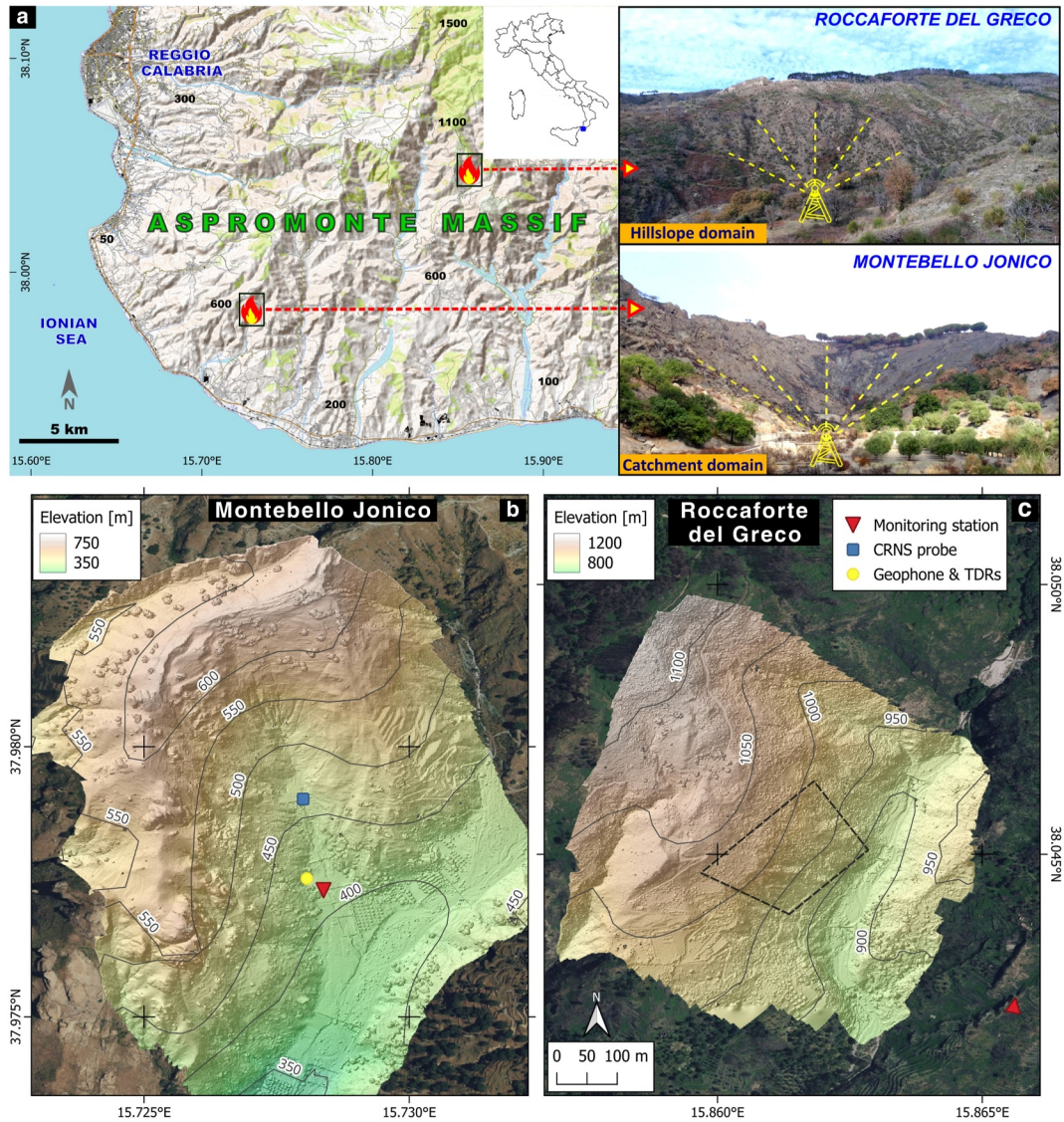


Figure 1. (a) Geographical context of the study area (background Open Street Map—EPSG 4326). The fire icons indicate the monitored sites represented in the pictures on the right. Approximate location of the monitoring stations and the field of view of the video cameras are indicated. (b) Digital surface model of the Montebello Jonico and (c) Roccaforte del Greco sites obtained with drone-based Lidar surveys. The dashed polygon in panel (c) identifies the monitored hillslope. In Roccaforte, the cosmic-ray neutron sensing probe and TDRs are installed at the same location as the monitoring station.

The ClimaVue™50 rainfall sensor is based on a drip counter that, in case of intense rainfall coupled with strong wind gusts, can be inaccurate. Therefore, we also installed a traditional tipping bucket rain gauge, NESA PL400, which is compliant with the World Meteorological Organization standards and guarantees higher reliability in terms of measurement range and accuracy of the triggering rainfall. Wind and lightning data are used to detect potential approaching storm cells and estimate their intensity.

3.3. Soil Water Content Sensors

The SWC is surveyed with two different methods. The first one is the cosmic-ray neutron sensing (CRNS) technology (Zreda et al., 2008) implemented by Finapp s.r.l. (Gianessi et al., 2024), which returns one SWC value per hour. A CRNS probe has the advantage of acquiring data from the neighboring area, up to a few hundred meters, and has penetration depth that varies between 15 and 83 cm below the sensor for wet and dry soil, respectively (Köhli et al., 2015). In Roccaforte, the CRNS probe is anchored to the main framework, whereas in

19448007, 2025, 19, Downloaded from https://agupubs.onlinelibrary.wiley.com/doi/10.1029/2025GL118170 by CochraneItalia, Wiley Online Library on [14/10/2025]. See the Terms and Conditions (https://onlinelibrary.wiley.com/terms-and-conditions) on Wiley Online Library for rules of use; OA articles are governed by the applicable Creative Commons License

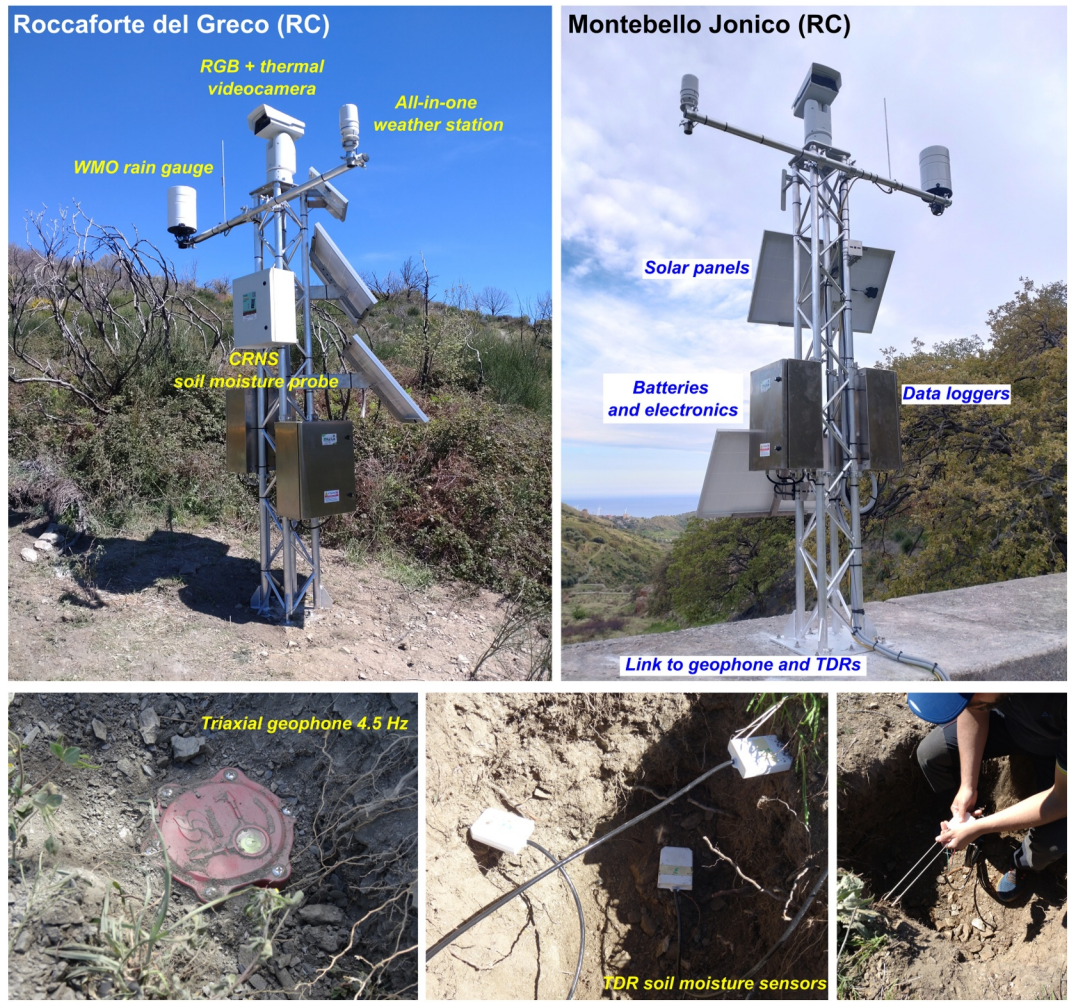


Figure 2. Photographs of the monitoring stations and details on the installation of the geophone (Montebello Jonico) and TDRs (Roccaforte del Greco).

Montebello, this is installed on a pole at 190 m of distance from the main station (Figure 1b), close to the source area of likely instability processes.

Besides the CRNS probe, we are employing three traditional TDR sensors (Campbell CS-650) in each site, to measure SWC and soil temperature with an acquisition rate of 10 min. In Montebello, all the TDRs are installed at 10 cm of depth at three different points on a hillslope nearby the main station. In Roccaforte, they are installed at 10, 20, and 45 cm on the same vertical profile below the CRNS probe (Figure 1c).

3.4. PTZ Bispectral Camera

An AXIS Q8752-E pan-tilt-zoom (PTZ) video camera acquiring visible and thermal videos simultaneously is installed in each site. The 800 × 600 px thermal sensor has fixed 35 mm lenses which guarantee high resolution at relatively long distances, and provides images 24/7. This sensor does not detect absolute temperatures of targets, but relative thermal variations into the scenes. The 1,920 × 1,080 px visible sensor is equipped with varifocal optical lens (from 4.3 to 137.6 mm) which can be robotically managed. When the camera is on, it continuously moves between established positions. At each position, the camera acquires short videos (8 s) at 1 frame per second at full resolution, which are instantaneously transmitted via FTP protocol to remote servers. This solution allows the thermal sensor to stabilize its own temperature, given that in the first 1–2 s of acquisition, the images present over or under exposure and geometric aberrations (Luhmann et al., 2020). Ordinarily, each camera is scheduled to power on every 4 hr, during which it acquires for 4 min. On the other hand, when the cumulative

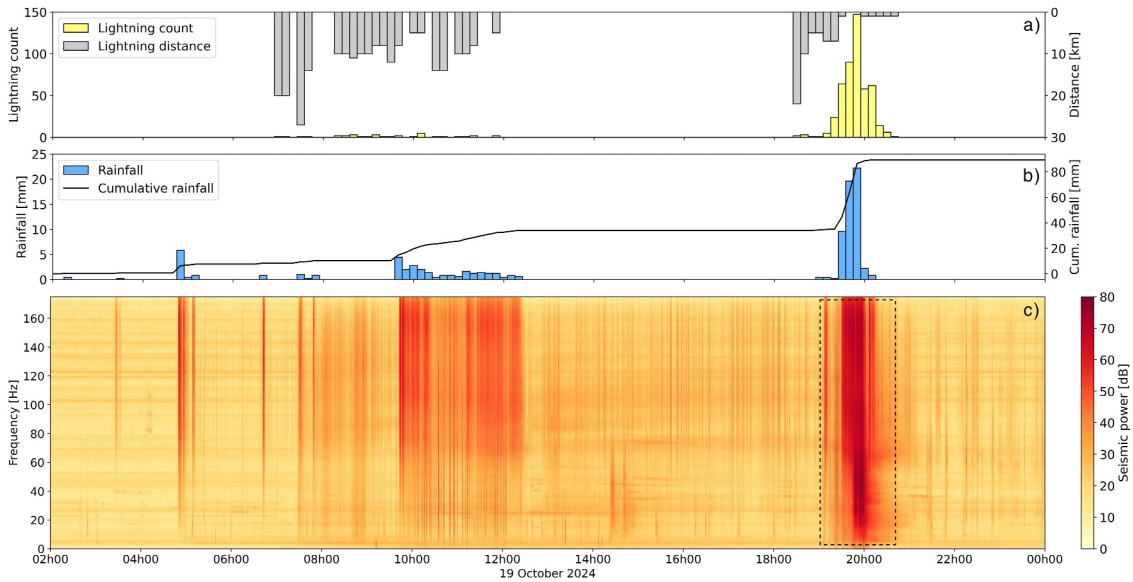


Figure 3. Charts showing data sets collected at the Montebello site: (a) 10-min lightning count and distance, (b) 10-min and cumulative rainfall, and (c) seismic power spectral density; the dashed rectangle outlines the period when the rainstorm and sediment-laden flow occurred. A focus on this period is shown in Figure S1.

rainfall exceeds 1 mm in 5 min or 12 mm in 3 hr, the camera is automatically kept on for the whole duration of the rainfall event and up to 1 hr after the rainfall has ended. All videos stored at remote servers are processed in real time to: (a) extract the last frame of each video, (b) coregister it by using the LAMMA algorithm (Dematteis et al., 2022), and (c) apply chromatic adjustments aimed at improving post-acquisition analyses.

3.5. Seismic Station

At Montebello station, we deployed seismic instrumentation to detect the signal associated with the potential activation of geomorphic processes. It consists of a Sunfull PS-4.5C1 4.5-Hz triaxial geophone, coupled with a DiGOS DATA-CUBE3 datalogger. Seismic data are continuously recorded at a sampling frequency of 400 Hz for the three components (one vertical and two horizontal) and synchronized with the other sensors through an external GPS antenna. In this configuration, we collect ∼500 MB of data each day. After each download, we compute the power spectral density to explore the temporal evolution and frequency content of the seismic signal. We do so over time windows of 15 s by performing a fast Fourier transform with the Welch's averaging method (Welch, 1967). In this study, we focus on the vertical component of the seismic signal.

4. Results

After the installation of the two stations in April 2024, we registered several intense rainfall events. The most impactful occurred on 19–21 October 2024 in Montebello, and on 17 January 2025 in Roccaforte (Esposito et al., 2025). Both events triggered geomorphic processes useful to evaluate the performance of the installed system.

4.1. Rainstorm in Montebello Jonico

Between 19 and 21 October 2024, more than 120 mm of rain fell in 60 hr over the Montebello catchment, of which approximately 50 mm in 30 min, between 19 hr 30 and 20 hr 00 (local time, UTC + 2) of 19 October. In that time, the rainfall was associated with a storm cell coming from the Ionian Sea, as confirmed by the wind direction (∼300°N). Starting at 18 hr 30, the lightning detector measured an increasing amount of lightning moving toward the sensor (Figure 3a). Accordingly, a 10-min peak of 147 lightning strikes at null distance (0 km) was measured at 19 hr 50. Overall, 295 lightings were detected within a range of 1 km from the sensor during the 30-min peak rainfall, such as when the storm cell impacted the Montebello catchment. Rainfall (Figure 3b) reached peak intensities in 1, 10, and 15 min of 168, 133, and 129 mm/hr, respectively (at 19 hr 58), determining a rapid increase of the SWC. At 10 cm soil depth, TDR measurements revealed that the SWC increased from 19% to 32%

19448007, 2025, 19, Downloaded from https://agupubs.onlinelibrary.wiley.com/doi/10.1029/2025GL118170 by CochraneItalia, Wiley Online Library on [14/10/2025]. See the Terms and Conditions (https://onlinelibrary.wiley.com/terms-and-conditions) on Wiley Online Library for rules of use; OA articles are governed by the applicable Creative Commons License

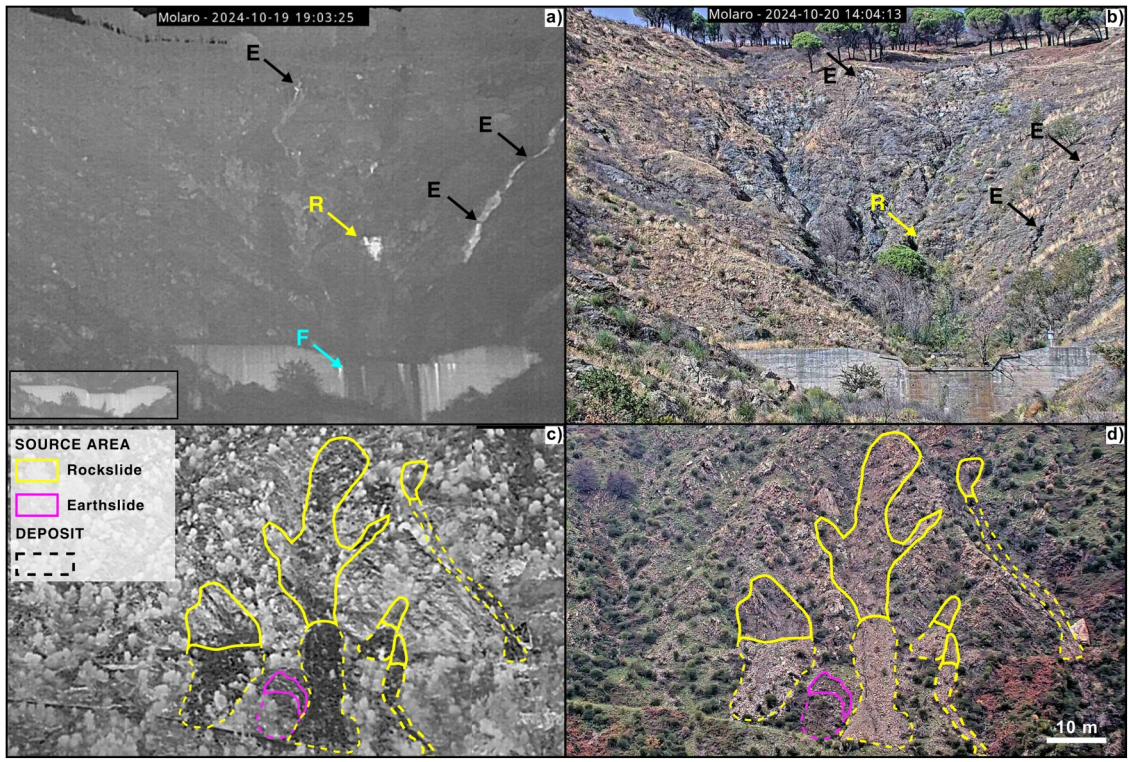


Figure 4. (a) Thermal and (b) visible images acquired at the Montebello site during and after the event of 19 October 2024 (date and UTC + 1 time of acquisition are labeled into the pictures). Geomorphic processes are indicated with letters: "E" gully erosion, "R" rockfall, and "F" sediment-laden flow over the check dam. The inset in panel (a) shows the check dam in ordinary (i.e., no flow) conditions. (c) Thermal and (d) visible diurnal images acquired at the Roccaforte site on 18 January 2025 (i.e., after the event of 17 January 2025). Different mass movements caused by the rainfall are outlined by differentiating source areas and deposits. The rockslide on the left is also shown during its occurrence in Movie S1, as well as the central and largest one in Movie S2. Further mass movements (not shown here) occurred nearby.

in these 30 min, whereas the CNRS probe recorded a SWC of 12% at 20 hr 00 and an hourly peak of 15% at 09 hr 00 on 20 October 2024. It is worth noting that on 18 October, the pre-event SWC was 4% as measured by both TDRs and the CRNS probe, indicating thus dry surface conditions.

The evolution of the rainstorm was also captured by the seismic station (Figure 3c), which detected peaks of seismic power of varying magnitude at high frequencies (i.e., 60–120 Hz), depending on rainfall intensity as reported in other studies (Bakker et al., 2022; Dean, 2017). In addition, between 19 hr 30 and 20 hr 00 a strong increase in seismic power is also visible at relatively low frequencies (i.e., 10–60 Hz in Figure 3c and Figure S1), which are typical of sediment-laden flows (Bakker et al., 2020). The flow initiated approximately 15 min after the onset of the rain burst and continued for at least 20 min after the rain ended (Figure S1).

By means of thermal images, we had the opportunity of detecting different geomorphic processes during their occurrence at night, even though heavy rainfall and thick fog obscured the thermal visibility for a few minutes. Interpretation of thermal images allowed us to recognize widespread gully erosion, a rockfall, and a turbulent flow presumably with high sediment concentration (Figure 4).

4.2. Daily Intense Rainfall in Roccaforte

On 17 January 2025, persistent rainfall occurred at Roccaforte leading to an amount of 172 mm in 24 hr, with a hourly peak intensity of 37 mm/hr (Figure 5). During the event, very strong wind gusts caused the loss of wind speed data. The rain sensor of the ClimaVue™50 suffered such conditions and its measurements diverged by those of the NESA PL400, which proved to be more reliable in that situation.

The three TDRs reacted to the rainfall input with a progressive increase of SWC, which was faster for those at 10 and 20 cm compared to the deepest at 45 cm (Figure 5). As expected, in correspondence of the most intense rain

19448007, 2025, 19, Downloaded from https://agupubs.onlinelibrary.wiley.com/doi/10.1029/2025GL118170 by CochraneItalia, Wiley Online Library on [14/10/2025]. See the Terms and Conditions (https://onlinelibrary.wiley.com/terms-and-conditions) on Wiley Online Library for rules of use; OA articles are governed by the applicable Creative Commons License

19448007, 2025, 19, Downloaded from https://agupubs.onlinelibrary.wiley.com/doi/10.1029/2025GL118170 by CochraneItalia, Wiley Online Library on [14/10/2025]. See the Terms and Conditions (https://onlinelibrary.wiley.com/terms-and-conditions) on Wiley Online Library for rules of use; OA articles are governed by the applicable Creative Commons License

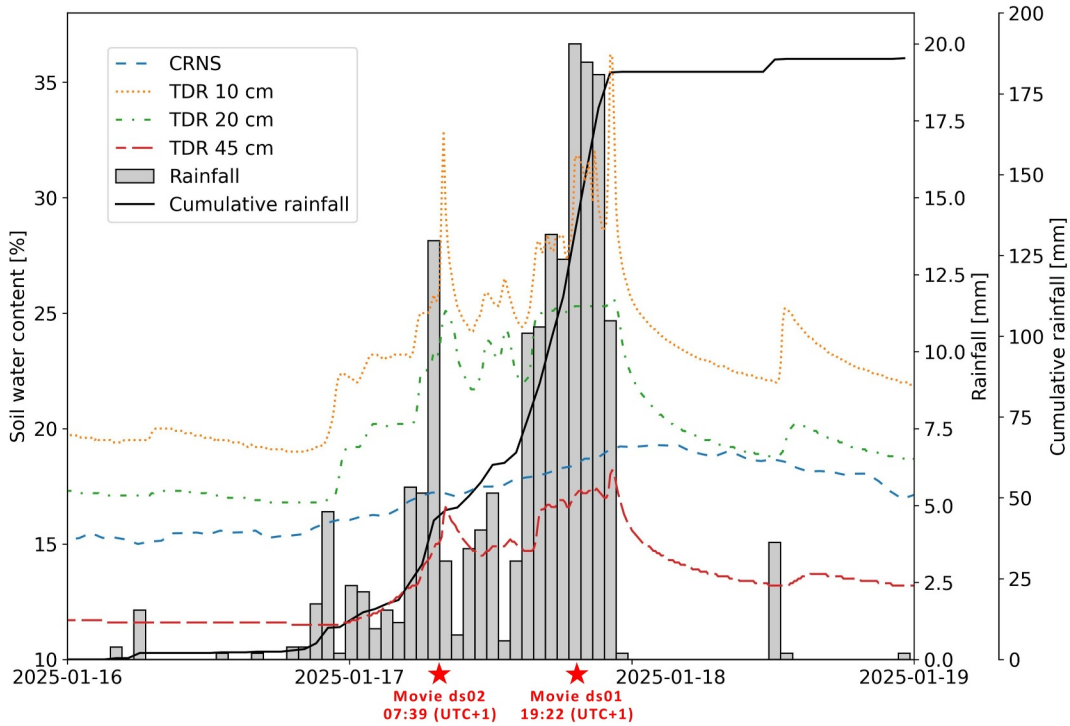


Figure 5. One-hour soil water content (SWC) measured by the cosmic-ray neutron sensing probe, and 10-min SWC measured by the TDR sensors at different depths. The 1-hr and cumulative rainfall collected from 16 to 19 January 2025 is also shown. The stars indicate the triggering time of rockslides shown in Movies S1 and S2.

bursts, the shallowest sensor at 10 cm recorded more pronounced 10-min peaks, with SWC values up to 36%. The CRNS probe also recorded an increasing SWC trend that reached a peak of 19% in the first hours of 18 January.

The long-lasting behavior of the heavy rainfall promoted rainwater infiltration, fostering in turn a general instability of the monitored hillslope. The activation of several mass movements was observed by means of thermal imagery, thanks to the strong thermal contrast between the substratum, left bare by the displaced material, and the surrounding stable hillslope (Movies S1 and S2). Visible images collected in the aftermath allowed classifying the mass movements as rock and earth slides (Figure 4). All of them initiated by displacing shallow material, between 0.5 and 1 m in thickness (e.g., Thomas et al., 2025), as assessed by means of a post-event drone-based lidar survey executed on 22 January 2025.

5. Discussion

The multi-sensor monitoring system presented in this work successfully allowed us to characterize important environmental conditions before and during two intense rainfall events triggering post-fire geomorphic processes. Specifically, by coupling rainfall and SWC sensors we observed how SWC responded to rainfall inputs, at high temporal resolution and from a three-dimensional perspective. Measurement of the lightning count and distance with 10-min time resolution allowed identifying a storm cell about 1 hr before approaching the Montebello catchment. Here, the seismic station proved to be very effective for defining the exact triggering and evolution times of the storm and sediment-laden flows in the main channel. Future developments may reveal also information about the flow magnitude and velocity (e.g., Porter et al., 2023).

At the same time, thermal images permitted to observe the activation of hillslope instabilities even when they occurred at night (Movies S1). It is worth noting that these images were very useful also in daylight conditions (Movie S2), demonstrating to be complementary to visible images for mapping purposes. In fact, areas affected by displacement of soil and rocks displayed a clear thermal signature that was different from the unaltered surface. This is evident in Montebello (Figure 4); in the images acquired at night during the rainfall, the hillslope surface had a homogeneous and colder temperature due to the rainfall, whereas the underlying dryer layer left exposed by

19448007, 2025, 19, Downloaded from https://agupubs.onlinelibrary.wiley.com/doi/10.1029/2025GL118170 by CochraneItalia, Wiley Online Library on [14/10/2025]. See the Terms and Conditions (https://onlinelibrary.wiley.com/terms-and-conditions) on Wiley Online Library for rules of use; OA articles are governed by the applicable Creative Commons License

the displaced soil and rock mass was warmer, and appeared much brighter. In Roccaforte, the Movie S2 documenting a rockslide during its occurrence, had a similar thermal signature. After the event, the deposited material appeared colder (i.e., darker) during the day (Figure 4), probably because it was wetter than the unaltered areas, or because the air circulating within the voids of coarse debris caused cooling for evaporation (Frodella et al., 2017). Relative thermal variations were observed in studies based on ground and drone-carried thermal infrared cameras, dealing with rockfall, and deep-seated landslides (Guerin et al., 2019; Vivaldi et al., 2023; Wellman et al., 2024). However, to our knowledge, thermal patterns related to the near real time occurrence of surface erosion and shallow landslides have never been documented so far.

Overall, geomorphic processes detected at the two pilot sites are similar to those observed in other post-fire settings worldwide (Moody et al. (2013) and references therein). Our observations suggest that gully erosion is very sensitive to high-intensity short-duration rainfall, especially in dry soil conditions leading to a likely reduction of water infiltration capacity (Vanmaercke et al., 2021; Yang et al., 2024). On the other hand, the initiation of rock and earth slides is associated with relatively high SWC conditions in the layers around 20–30 cm (Figure 5). In both sites we measured maximum SWC peaks below 50%, meaning that hillslope instabilities occurred in partially saturated conditions.

6. Conclusions

In this study, we monitored in real time two sites prone to post-fire geomorphic processes, using advanced technologies consisting of autonomous all-in weather stations, TDR and CRNS SWC sensors, visible and thermal video cameras, and a seismic station. The experimented technologies proved to be effective for reaching the research goals, overcoming some limitations affecting traditional instrumentation. Different types of instability processes generated by two rainfall events were fully characterized in terms of predisposing and triggering conditions, as well as timely detected even during the night. The outcomes of this study offer new solutions that could be applied also in other sites to improve existing knowledge about initiation mechanisms of post-fire geomorphic processes that, as known, can develop in very short times (i.e., less than 30 min) endangering people and properties. Modularity allows the monitoring system to be customized and adapted for other specific contexts. In the Montebello site, we plan to add further instruments for improving the monitoring capacities of both initiation areas and the main channel (i.e., flow propagation and magnitude), like pressure transducers, stream stage sensors, accelerometers, and other cameras to investigate possible bed failure mechanisms. In the end, heterogeneity and quality of information collected by multi-sensor systems like this may support also early warning actions.

Conflict of Interest

The authors declare no conflicts of interest relevant to this study.

Data Availability Statement

Data sets associated with this manuscript are available under CC-BY 4.0 license on the Zenodo repository (Esposito et al., 2025).

Acknowledgments

This work was funded by the Next Generation EU—Italian NRRP, Mission 4, Component 2, Investment 1.5, call for the creation and strengthening of "Innovation Ecosystems," building "Territorial R&D Leaders" (Directorial Decree 2021/3277) —project Tech4You—Technologies for climate change adaptation and quality of life improvement, ECS0000009. This work reflects only the authors' views and opinions, neither the Ministry for University and Research nor the European Commission can be considered responsible for them. We thank Dr. Tommaso Moramarco (CNR IRPI) for providing all the necessary support to realize the research activity, and Prof. Pasquale Marziliano (Università degli Studi Mediterranea di Reggio Calabria) for his kind assistance in the field. We also thank the Hortus s.r.l. and Finapp s.r.l. companies that provided all the instrumentation. A great support was given by Paolo Calabrò (Comune di Montebello Jonico) and Francesco Saccà (Azienda Agricola Saccà, Roccaforte del Greco) that helped us in the installation activities. The authors express our sincerest gratitude to the late Dr. Velio Coviello, who participated in the preliminary design of the monitoring system with valuable ideas and suggestions. The authors acknowledge the comments from David B. Cavagnaro and another anonymous Reviewer which helped to improve the content, quality, and readability of the work. Open access publishing facilitated by Consiglio Nazionale delle Ricerche, as part of the Wiley - CRUI-CARE agreement.

References

Bakker, M., Gimbert, F., Geay, T., Misset, C., Zanker, S., & Recking, A. (2020). Field application and validation of a seismic bedload transport model. *Journal of Geophysical Research: Earth Surface*, *125*(5), e2019JF005416. https://doi.org/10.1029/2019JF005416

Bakker, M., Legout, C., Gimbert, F., Nord, G., Boudevillain, B., & Freche, G. (2022). Seismic modelling and observations of rainfall. *Journal of Hydrology*, *610*, 127812. https://doi.org/10.1016/j.jhydrol.2022.127812

Bombino, G., Barbaro, G., D'Agostino, D., Denisi, P., Foti, G., & Zimbone, S. M. (2024). Relationships between torrent check dam systems and shoreline dynamics in semi-arid Mediterranean area: A sub-regional focus in Calabria, Italy. *Geomorphology*, *458*, 109259. https://doi.org/10.1016/j.geomorph.2024.109259

Bombino, G., D'Agostino, D., Marziliano, P. A., Pérez Cutillas, P., Praticò, S., Proto, A. R., et al. (2024). A nature-based approach using felled burnt logs to enhance forest recovery post-fire and reduce erosion phenomena in the Mediterranean area. *Land*, *13*(2), 236. https://doi.org/10.3390/land13020236

Calcaterra, D., & Parise, M. (2010). Weathering in the crystalline rocks of Calabria, Italy, and relationships to landslides. *Geological Society, London, Engineering Geology Special Publications*, *23*(1), 105–130. https://doi.org/10.1144/EGSP23.7

Cao, X., He, K., Hu, X., Luo, G., Zhou, Y., Zhou, R., et al. (2024). Combined InSAR and optical dataset unravelling the characteristics of hillslope erosion in burned areas in Xichang, China. *Catena*, *242*, 108123. https://doi.org/10.1016/j.catena.2024.108123

Dean, T. (2017). The seismic signature of rain. *Geophysics*, *82*(5), P53–P60. https://doi.org/10.1190/geo2016-0421.1

Dematteis, N., Giordan, D., Crippa, B., & Monserrat, O. (2022). Fast local adaptive multiscale image matching algorithm for remote sensing image correlation. *Computers & Geosciences*, *159*, 104988. https://doi.org/10.1016/j.cageo.2021.104988

Ellett, N. G., Pierce, J. L., & Glenn, N. F. (2019). Partitioned by process: Measuring post-fire debris-flow and rill erosion with structure from motion photogrammetry. *Earth Surface Processes and Landforms*, *44*(15), 3128–3146. https://doi.org/10.1002/esp.4728

Esposito, G., Dematteis, N., Cavalli, R. M., Cavalli, M., Crema, S., De Biase, M., et al. (2025). In-situ monitoring datasets documenting two post-fire geomorphic responses in Calabria, southern Italy [Dataset]. *Zenodo*. https://doi.org/10.5281/zenodo.15862333

Esposito, G., Gariano, S. L., Masi, R., Alfano, S., & Giannatiempo, G. (2023). Rainfall conditions leading to runoff-initiated post-fire debris flows in Campania, southern Italy. *Geomorphology*, *423*, 108557. https://doi.org/10.1016/j.geomorph.2022.108557

Frodella, W., Gigli, G., Morelli, S., Lombardi, L., & Casagli, N. (2017). Landslide mapping and characterization through infrared thermography (IRT): Suggestions for a methodological approach from some case studies. *Remote Sensing*, *9*(12), 1281. https://doi.org/10.3390/rs9121281

Gartner, J. E., Cannon, S. H., Bigio, E. R., Davis, N. K., Parrett, C., Pierce, K. L., et al. (2005). Compilation of data relating to the erosive response of 608 recently-burned basins in the western United States. *US Geological Survey*.

Gianessi, S., Polo, M., Stevanato, L., Lunardon, M., Francke, T., Oswald, S. E., et al. (2024). Testing a novel sensor design to jointly measure cosmic-ray neutrons, muons and gamma rays for non-invasive soil moisture estimation. *Geoscientific Instrumentation, Methods and Data Systems*, *13*(1), 9–25. https://doi.org/10.5194/gi-13-9-2024

González-Pelayo, O., Prats, S. A., Van Den Elsen, E., Malvar, M. C., Ritsema, C., Bautista, S., & Keizer, J. J. (2024). The effects of wildfire frequency on post-fire soil surface water dynamics. *European Journal of Forest Research*, *143*(2), 493–508. https://doi.org/10.1007/s10342-023-01635-z

Guerin, A., Jaboyedoff, M., Collins, B. D., Derron, M.-H., Stock, G. M., Matasci, B., et al. (2019). Detection of rock bridges by infrared thermal imaging and modeling. *Scientific Reports*, *9*(1), 13138. https://doi.org/10.1038/s41598-019-49336-1

Hürlimann, M., Coviello, V., Bel, C., Guo, X., Berti, M., Graf, C., et al. (2019). Debris-flow monitoring and warning: Review and examples. *Earth-Science Reviews*, *199*, 102981. https://doi.org/10.1016/j.earscirev.2019.102981

Kean, J. W., Staley, D. M., & Cannon, S. H. (2011). In situ measurements of post-fire debris flows in southern California: Comparisons of the timing and magnitude of 24 debris-flow events with rainfall and soil moisture conditions. *Journal of Geophysical Research*, *116*(F4), F04019. https://doi.org/10.1029/2011JF002005

Kean, J. W., Staley, D. M., Leeper, R. J., Schmidt, K. M., & Gartner, J. E. (2012). A low-cost method to measure the timing of postfire flash floods and debris flows relative to rainfall: Measuring timing of postfire flash floods. *Water Resources Research*, *48*(5), W05516. https://doi.org/10.1029/2011WR011460

Köhli, M., Schrön, M., Zreda, M., Schmidt, U., Dietrich, P., & Zacharias, S. (2015). Footprint characteristics revised for field-scale soil moisture monitoring with cosmic-ray neutrons. *Water Resources Research*, *51*(7), 5772–5790. https://doi.org/10.1002/2015WR017169

Luhmann, T., Robson, S., Kyle, S., & Boehm, J. (2020). *Close-range photogrammetry and 3D imaging*. Walter de Gruyter GmbH & Co KG.

Martinez, J. R., McGuire, L. A., & Youberg, A. M. (2025). Insights into temporal changes in debris flow susceptibility following fire in the southwest USA from monitoring and repeat estimates of soil hydraulic and physical properties. *Earth Surface Processes and Landforms*, *50*(2), e70015. https://doi.org/10.1002/esp.70015

Moody, J. A., Shakesby, R. A., Robichaud, P. R., Cannon, S. H., & Martin, D. A. (2013). Current research issues related to post-wildfire runoff and erosion processes. *Earth-Science Reviews*, *122*, 10–37. https://doi.org/10.1016/j.earscirev.2013.03.004

Ouyang, C., Xiang, W., An, H., Wang, F., Yang, W., & Fan, J. (2023). Mechanistic analysis and numerical simulation of the 2021 post-fire debris flow in Xiangjiao catchment, China. *Journal of Geophysical Research: Earth Surface*, *128*(1), e2022JF006846. https://doi.org/10.1029/2022JF006846

Pelletier, J. D., & Orem, C. A. (2014). How do sediment yields from post-wildfire debris-laden flows depend on terrain slope, soil burn severity class, and drainage basin area? Insights from airborne-LiDAR change detection: POST-FIRE sediment yields measured by airborne lidar. *Earth Surface Processes and Landforms*, *39*(13), 1822–1832. https://doi.org/10.1002/esp.3570

Porter, R., Joyal, T., Beers, R., Loverich, J., LaPlante, A., Spruell, J., et al. (2021). Seismic monitoring of post-wildfire debris flows following the 2019 Museum fire, Arizona. *Frontiers in Earth Science*, *9*, 649938. https://doi.org/10.3389/feart.2021.649938

Porter, R., Joyal, T., Beers, R., Youberg, A., Loverich, J., Schenk, E., & Robichaud, P. R. (2023). Characterization of environmental seismic signals in a post-wildfire environment: Examples from the Museum fire, AZ. *Journal of Geophysical Research: Earth Surface*, *128*(7), e2022JF006962. https://doi.org/10.1029/2022JF006962

Raymond, C. A., McGuire, L. A., Youberg, A. M., Staley, D. M., & Kean, J. W. (2020). Thresholds for post-wildfire debris flows: Insights from the Pinal Fire, Arizona, USA. *Earth Surface Processes and Landforms*, *45*(6), 1349–1360. https://doi.org/10.1002/esp.4805

Rengers, F. K., McGuire, L. A., Kean, J. W., Staley, D. M., & Youberg, A. M. (2019). Progress in simplifying hydrologic model parameterization for broad applications to post-wildfire flooding and debris-flow hazards. *Earth Surface Processes and Landforms*, *44*(15), 3078–3092. https://doi.org/10.1002/esp.4697

Robustelli, G., & Sorriso-Valvo, M. (2017). The landscape of the Aspromonte Massif: A geomorphological open-air laboratory. In M. Soldati & M. Marchetti (Eds.), *Landscapes and landforms of Italy* (pp. 431–441). Springer International Publishing. https://doi.org/10.1007/978-3-319-26194-2_37

Tang, H., McGuire, L. A., Rengers, F. K., Kean, J. W., Staley, D. M., & Smith, J. B. (2019). Evolution of debris-flow initiation mechanisms and sediment sources during a sequence of postwildfire rainstorms. *Journal of Geophysical Research: Earth Surface*, *124*(6), 1572–1595. https://doi.org/10.1029/2018JF004837

Thomas, M. A., Lindsay, D. N., Kean, J. W., Graber, A. P., Rossi, R. K., Kostelnik, J., et al. (2025). Landsliding follows signatures of wildfire history and vegetation regrowth in a steep coastal shrubland. *Geosphere*, *21*(5), 823–840. https://doi.org/10.1130/GES02856.1

Vanmaercke, M., Panagos, P., Vanwalleghem, T., Hayas, A., Foerster, S., Borrelli, P., et al. (2021). Measuring, modelling and managing gully erosion at large scales: A state of the art. *Earth-Science Reviews*, *218*, 103637. https://doi.org/10.1016/j.earscirev.2021.103637

Vivaldi, V., Bordoni, M., Mineo, S., Crozi, M., Pappalardo, G., & Meisina, C. (2023). Airborne combined photogrammetry—infrared thermography applied to landslide remote monitoring. *Landslides*, *20*(2), 297–313. https://doi.org/10.1007/s10346-022-01970-z

Welch, P. (1967). The use of fast Fourier transform for the estimation of power spectra: A method based on time averaging over short, modified periodograms. *IEEE Transactions on Audio and Electroacoustics*, *15*(2), 70–73. https://doi.org/10.1109/TAU.1967.1161901

Wellman, E. C., Schafer, K. W., Williams, C. P., Ojum, G. H., Potter, J. J., Brown, L. D., et al. (2024). Observation of rockfall in the thermal infrared. *Rock Mechanics and Rock Engineering*. https://doi.org/10.1007/s00603-024-04254-1

Yang, H., Liu, J., Sun, H., You, Y., Zhao, W., & Yang, D. (2024). Evolution characteristics of post-fire debris flow in Xiangjiao Gully, Muli County. *Catena*, *246*, 108353. https://doi.org/10.1016/j.catena.2024.108353

Zreda, M., Desilets, D., Ferré, T. P. A., & Scott, R. L. (2008). Measuring soil moisture content non-invasively at intermediate spatial scale using cosmic-ray neutrons. *Geophysical Research Letters*, *35*(21), 2008GL035655. https://doi.org/10.1029/2008GL035655

19448007, 2025, 19, Downloaded from https://agupubs.onlinelibrary.wiley.com/doi/10.1029/2025GL118170 by CochraneItalia, Wiley Online Library on [14/10/2025]. See the Terms and Conditions (https://onlinelibrary.wiley.com/terms-and-conditions) on Wiley Online Library for rules of use; OA articles are governed by the applicable Creative Commons License